

CS-based Lung Covid-Affected X-Ray Image Disorders Classification using Convolutional Neural Network

Biyanika Emili Triasari¹, Gelar Budiman², Siti Sarah Maidin³, M. Izham Jaya⁴,
Yuli Sun Hariyani⁵, Indrarini Dyah Irawati^{6,*}, Zhong Zhao⁷

^{1,2}*School of Electrical Engineering, Telkom University, Indonesia*

³*Faculty of Data Science & Information Technology, INTI International University, Malaysia*

⁴*Faculty of Computing, Universiti Malaysia Pahang Al-Sultan Abdullah, Malaysia*

^{5,6}*School of Applied Science, Telkom University, Indonesia*

⁷*Faculty of Liberal Arts, Shinawatra University, Thailand*

(Received: June 13, 2024; Revised: July 18, 2024; Accepted: August 23, 2024; Available online: November 7, 2024)

Abstract

Lung diseases, such as pneumonia, significantly affect the respiratory system, especially the lungs. This condition causes various degrees of lung damage in patients of all age groups, including the elderly, adults, and children. Even after treatment and recovery, diagnosing lung damage remains important, which can be done using rapid tests, clinical evaluations, CT scans, or X-rays. This study focuses on the classification of X-ray images of lungs affected by pneumonia and normal lungs, using the Convolutional Neural Network method based on Compressive Sensing (CS) simulated using MatLab. The purpose of the study is to determine the performance by calculating the confusion matrix value. The number of datasets used for normal lungs and those affected by pneumonia is 300 X-ray images from several different sources, with 60% training data, 30% validation, and 10% testing. The addition of the compression process causes a decrease in image quality, expressed in PSNR, as well as a decrease in classification parameters such as accuracy. Compared with previous research, the system without compression produces the highest accuracy. The results of the study can help classify lungs affected by pneumonia.

Keywords: Classification, Compressive Sensing, Convolutional Neural Network, X-ray, Inclusive Health, Process Innovation

1. Introduction

Lung infections, such as pneumonia, present significant health challenges that can severely impact the human respiratory system. These infections may lead to conditions like lung fibrosis and acute respiratory distress syndrome (ARDS), resulting in reduced lung capacity and difficulty breathing. Pneumonia, in particular, causes inflammation and fluid buildup in the alveoli, leading to shortness of breath, persistent cough, and long-term respiratory issues. Early detection and monitoring are crucial for preventing further complications and improving recovery [1], [2].

Numerous studies have been conducted to detect abnormalities in chest X-rays using Machine and Deep Learning techniques [3], [4]. In [5], pneumonia was detected based on X-ray images using the Deep Residual Network with the Resnet50 method, achieving an accuracy of 99%, precision of 98%, recall of 95%, and an F1-score of 97%. Another study applied the Deep Learning Transfer Model with an Ensemble Method, resulting in medical image classification with an accuracy of 98%, precision of 98.66%, and an F1-score of 98.30% [6]. Research concluded that the best performance in CT scan image classification of lung diseases was obtained by extracting features using GLCM, GLSZM, and DWT methods, achieving classification accuracy exceeding 90% with 10-fold cross-validation [7]. Similarly, pneumonia detection using chest X-ray images with the Resnet 101 method achieved image classification accuracy of 99.4%, precision of 98.7%, recall of 99.2%, and an F1-score of 99% [8]. CNN hyperparameter tuning was

*Corresponding author: Indrarini Dyah Irawati (indrarini@telkomuniversity.ac.id)

DOI: <https://doi.org/10.47738/jads.v5i4.371>

This is an open access article under the CC-BY license (<https://creativecommons.org/licenses/by/4.0/>).

© Authors retain all copyrights

applied in detecting lung infections from X-rays and CT scans, resulting in accuracy, precision, recall, and F1-scores of over 94% [9]. Furthermore, segmentation and classification techniques were combined using the Deep Residual U-Net (DrU-Net) architecture for lung disease detection [10]. Another approach involved deep feature extraction using CNN and feature detection with long short-term memory (LSTM) to automatically diagnose lung infections from 4575 X-ray images [11].

In this study, we detect lung infections based on chest X-ray images. This early detection system is essential for preventing severe impacts on the lungs caused by infections. Our research combines Compressive Sensing (CS) techniques to reduce file sizes [12] and Convolutional Neural Networks (CNN) to classify lung conditions. The CS method utilizes the DCT algorithm as a sparsifying technique, random Gaussian as a measurement matrix, and the OMP algorithm for reconstruction [13], [14]. This study uses CNN with the AlexNet architecture.

Supporting Sustainable Development Goal (SDG) 3, which focuses on ensuring healthy lives and promoting well-being for all ages, involves leveraging technological advancements to improve health outcomes. This study contributes to SDG 3 by integrating advanced machine learning techniques to develop diagnostic tools for medical professionals and students. By simulating these methods using MATLAB, the study advances medical imaging analysis and provides a valuable resource for enhancing diagnostic capabilities. By aligning with SDG 3, this research improves healthcare quality by offering practical applications of theoretical knowledge, fostering better understanding and innovation. Ultimately, this contributes to building a knowledgeable and skilled healthcare workforce capable of addressing current and future health challenges [15].

2. Literature Review

Lung infections, particularly pneumonia, represent a significant health burden worldwide. These infections can lead to severe complications such as lung fibrosis and acute respiratory distress syndrome (ARDS), which impair lung function and reduce respiratory capacity. The inflammation and fluid accumulation in the alveoli caused by pneumonia result in symptoms like shortness of breath, persistent cough, and long-term respiratory complications. Therefore, early detection and continuous monitoring of lung infections are essential to mitigate severe outcomes and promote effective recovery [16], [17].

Advancements in Machine Learning (ML) and Deep Learning (DL) have significantly improved the capability to detect and diagnose lung conditions from medical images. Research has shown that ML and DL techniques can effectively identify abnormalities in chest X-rays and CT scans, making them valuable tools for early diagnosis. For instance, a study using the Resnet50 deep residual network method successfully detected pneumonia from X-ray images, achieving high accuracy and precision, thus demonstrating the potential of DL for reliable diagnosis [18]. Another approach utilized an ensemble method with deep learning transfer models, achieving robust classification accuracy and precision, further underscoring the benefits of advanced machine learning algorithms in medical diagnostics [19].

In addition to X-ray analysis, feature extraction methods have been developed to enhance the classification of lung diseases using CT scan images. Techniques such as Gray-Level Co-occurrence Matrix (GLCM), Gray-Level Size Zone Matrix (GLSZM), and Discrete Wavelet Transform (DWT) have been employed to improve feature extraction, resulting in classification accuracy above 90% with rigorous cross-validation methods [20]. Similarly, Resnet 101 has been used for pneumonia detection, achieving near-perfect classification accuracy, precision, and recall, which highlights the effectiveness of DL in medical image processing [21].

Moreover, studies have focused on optimizing neural networks through hyperparameter tuning to further improve diagnostic accuracy. For example, the application of Convolutional Neural Networks (CNN) in detecting lung infections from X-rays and CT scans has demonstrated performance metrics with accuracy, precision, recall, and F1-scores consistently exceeding 94% [22]. Additionally, segmentation and classification were combined using the Deep Residual U-Net (DrU-Net) architecture to enhance lung disease detection, which provides a comprehensive solution for segmenting infected areas and classifying diseases [23].

Some researchers have also integrated feature extraction with temporal sequence models such as long short-term memory (LSTM) to diagnose lung infections. This approach has been used to analyze a dataset of thousands of X-ray

images, successfully extracting features and diagnosing lung conditions automatically [24]. This integration demonstrates the potential of combining DL models for both feature extraction and pattern recognition in the diagnosis of complex diseases.

Apart from classification and feature extraction, Compressive Sensing (CS) techniques have been explored to reduce the file sizes of medical images without sacrificing diagnostic quality. By employing the Discrete Cosine Transform (DCT) algorithm as a sparsifying technique along with random Gaussian measurement matrices and Orthogonal Matching Pursuit (OMP) for reconstruction, researchers have managed to compress medical images effectively, thus facilitating faster data processing and analysis [18], [19].

Overall, the integration of advanced ML and DL techniques in diagnostic systems has shown great promise in improving the detection and management of lung infections. By combining various approaches, including segmentation, classification, feature extraction, and data compression, these technologies provide comprehensive solutions for early diagnosis, supporting the objectives of Sustainable Development Goal (SDG) 3, which aims to ensure healthy lives and promote well-being for all ages [21].

3. Methodology

This study employs a combination of CS techniques and CNN methods to classify lung X-ray images affected by lung infections, such as pneumonia. The primary objective is to utilize the CS technique to reduce the file size of X-ray images without significantly compromising their quality, followed by the application of CNN for accurate classification. The methodology section outlines the processes involved in data collection, image compression, and classification, providing a comprehensive overview of the steps taken to achieve the study's goals. These steps include the application of CS techniques to compress medical images, maintaining image integrity, and subsequently utilizing CNN for high-accuracy diagnosis of lung conditions based on the processed X-ray images. This integrated approach ensures that even with reduced image sizes, the system is capable of detecting lung abnormalities effectively, contributing to the advancement of medical image analysis techniques in the healthcare industry.

In the training and testing stages, the dataset undergoes a series of preprocessing steps, including sparsity and acquisition using CS methods, followed by image reconstruction. The images are then processed through a CNN with the Alexnet architecture to classify lung health. The performance of the system is evaluated using metrics such as accuracy, precision, recall, and F1-score. The figure 1 illustrates the overall process of the lung health classification system.

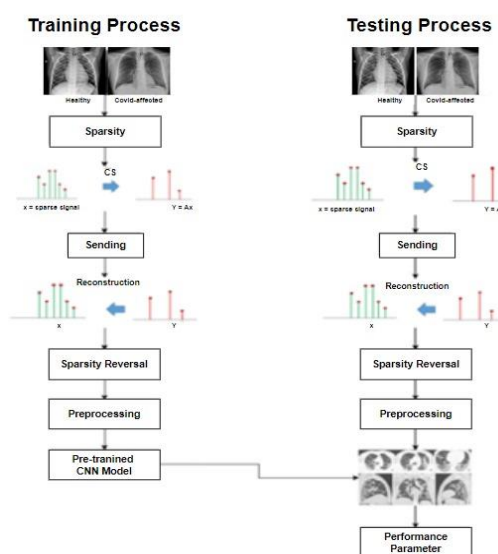


Figure 1. Block diagram for lung healthy classification system

The block diagram is divided into two processes: training and testing. The collection of X-ray dataset images of lungs infected with COVID-19 was obtained from <https://github.com/ieee8023/covid-chestxray-dataset/tree/master/images>,

while normal lungs were obtained from <https://data.mendeley.com/datasets/rscbjbr9sj/2>, as shown in figure 2. Chest X-rays are radiographic projections to find out the anatomical conditions in the thorax (chest) which includes the heart and lung organs using X-ray radiation. The dataset used for normal and COVID-19 infected lungs consists of 300 x-ray images with 60% for training data, 30% for validation, and 10% for testing.

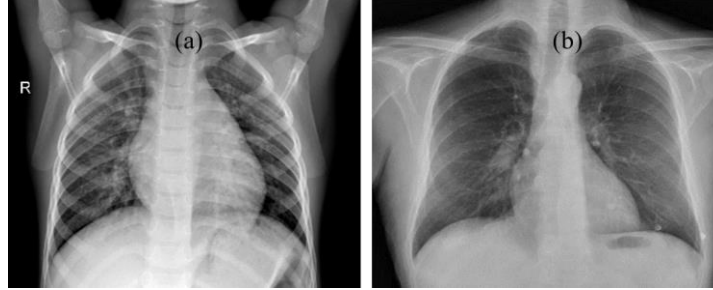


Figure 2. Datasets: (a) Mendeley dataset (b) github dataset

Simulation experiments using CS with DCT for sparsifying technique, OMP as reconstruction algorithm, and CNN as training method with Alexnet architecture. During the training and testing stages, the dataset enters the sparsity stage using the DCT technique which successfully compresses signals or images. After that, the signal sparsity results go into the CS acquisition stage using a measurement matrix generated randomly from a Gaussian normal distribution. The output in the form of a compression signal is used to calculate CS performance based on the Compression Ratio (CR) parameter. CR means the ratio of the compressed image size to the size of uncompressed image, as seen in equation (1). The compressed signal is sent from the sender to the receiver with the Compression Ratio (CR) as following:

$$CR = \frac{L_a}{L_b}, \quad (1)$$

where L_a is the length of signal after compression and L_b is the length of the signal before compression.

On the receiver side, to recover the sparse signal from the compressed signal and measurement matrix, a reconstruction algorithm is needed, in this case using OMP. This reconstructed signal is returned to the original signal through the Inverse DCT (IDCT) process. To determine the image quality due to the compression process, the PSNR parameter is used which compares the quality of the original image with the IDCT reconstructed image. The PSNR equation is shown in (2) as following:

$$PSNR = 10 \log_{10} \left(\frac{C_{max}}{MSE} \right), \quad (2)$$

$$MSE = \frac{1}{MN} \sum_{x=1}^M \sum_{y=1}^N (S_{xy} - C_{xy})^2, \quad (3)$$

where C_{max} is the largest pixel value in the whole image, x and y represent the coordinates of points in the image, M and N represent the image dimensions, S is the inserted image, and C is the original image.

The next activity is preprocessing using the CNN technique. The reconstructed image is resized to 256×256. Subsequently, the color of the image is changed from gray to RGB. This image undergoes processing through classification technique using CNN with Alexnet architecture. Alexnet is one of the CNN architectures that won the title at the ImageNet Large Scale Visual Recognition Challenge (ILSVRC) competition which is a large-scale image classification competition in 2012. AlexNet is a new breakthrough in deep learning by applying ConvsNet combined with Dropout Regularization technique, utilizing ReLu as activation function and data augmentation. Alexnet is designed to be able to perform classification with 1000 categories. Alexnet architecture consists of 5 convolution layers, 3 pooling layers, 2 dropout layers, and 3 fully connected layers. Evaluation is done by calculating the confusion matrix in the form of accuracy, precision, recall, and F1-score, to determine the performance obtained from the research.

4. Results and Discussion

The results and discussion section presents the findings of this study, which focuses on the classification of lung X-ray images affected by COVID-19 using a combination of CS and CNN with AlexNet architecture. This section provides

an analysis of the performance of the proposed system, including the impact of various compression ratios on image quality and classification accuracy. Key metrics such as Peak Signal-to-Noise Ratio (PSNR), accuracy, precision, recall, and F1-score are used to evaluate the effectiveness of the method. The results are compared with previous studies to highlight the advantages and limitations of the proposed approach.

3.1. Compressive Sensing

Table 1 shows the average PSNR value of the original image compared to the image resulting from the compression process. The experiment was carried out on 180 images. Testing was run for 6 scenarios, such as without compression (CR=0), CR 2, CR4, CR 8, CR 16 and CR 64. The results show that the CR of 2, has an average PSNR value of 32.914 for covid-affected lung images and 30.590 for healthy lung images. While the experiments using CR of 16, an average PSNR is still above 20 dB with a value of 23.252 dB for covid-affected lung images and 20.993 dB for healthy lung images. From these results, it can be concluded that CR and PSNR are inversely proportional, where the greater the CR, the smaller the PSNR or vice versa, the smaller the CR, the greater the PSNR.

Table 1. Average PSNR Values for Original and Compressed Images at Different Compression Ratios

CR	PSNR (dB)	
	Infected with Covid-19	Normal
64	16.737	11.510
32	21.796	18.546
16	23.252	20.993
8	24.240	22.366
4	27.715	25.457
2	32.914	30.590

Figure 3(a) and figure 3(b) show that the images compressed by the CR are not very clear, only a few images are visible. In figure 3(c) and figure 3(d) the image has started to look clear but there are still some images that look unclear. In figure 3(e) and figure 3(f) the image is clearly visible. It can be concluded that the greater the CR value, the worse the image quality.

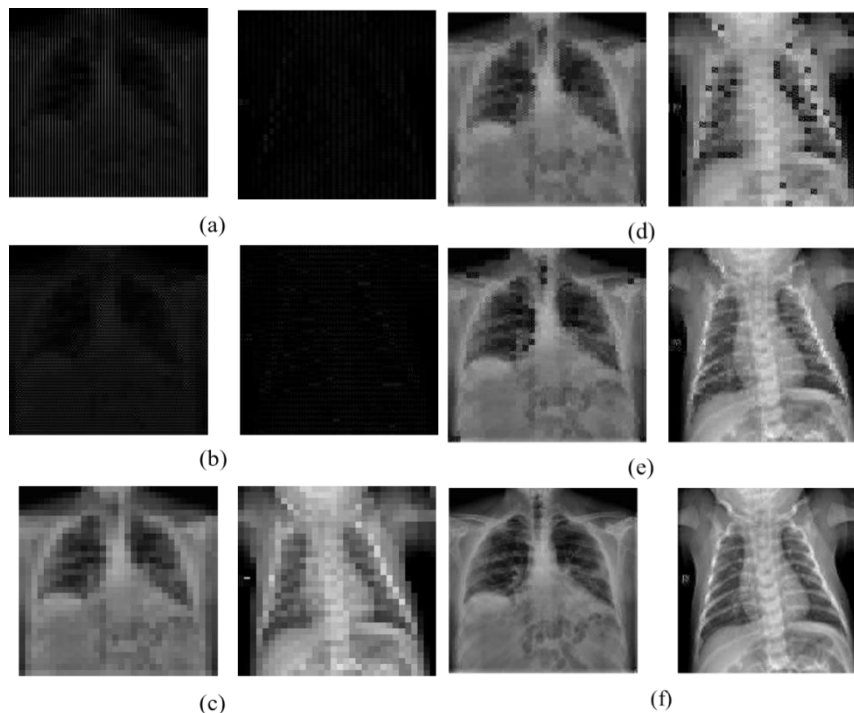


Figure 3. X-ray images of COVID19-affected (left) and healthy (right) lungs at compression ratios of (a) 64 (b) 32 (c) 16 (d) 8 (e) 4 and (f) 2

3.2. Training

In the training stage 180 images were used, while in the validation stage 90 images were used. Both processes are iterated until 30 epochs or the loss convergence. The optimization algorithm updates the network weights during training and validation by using the learning rate 0.0005. For all training experiments, accuracy was obtained at 100%. However, the validation value is different. In the experiment without prior compression and CR of 2, the validation value was 100%, as seen in figure 4. It can be concluded that the greater the compression ratio, the better the validation value.

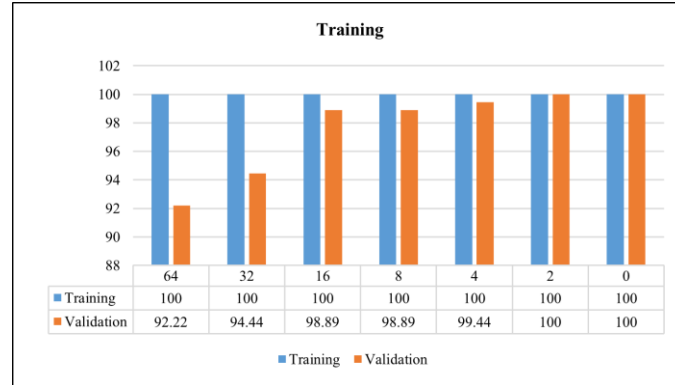


Figure 4. Training Accuracy and Validation Accuracy at Different Compression Ratios

3.3. Testing

Figure 5 shows the testing results using 30 images. The test results show that when the system does not use compression techniques or CR=0, all performance parameters, such as: accuracy, precision, recall and F1-score are worth 100%. For example, at CR=2, accuracy is 98.33, precision is 100%, recall is 96.67% and F1-score is 98.31%. In the application of CS, it can be concluded that the smaller the CR, the higher of all parameters value.

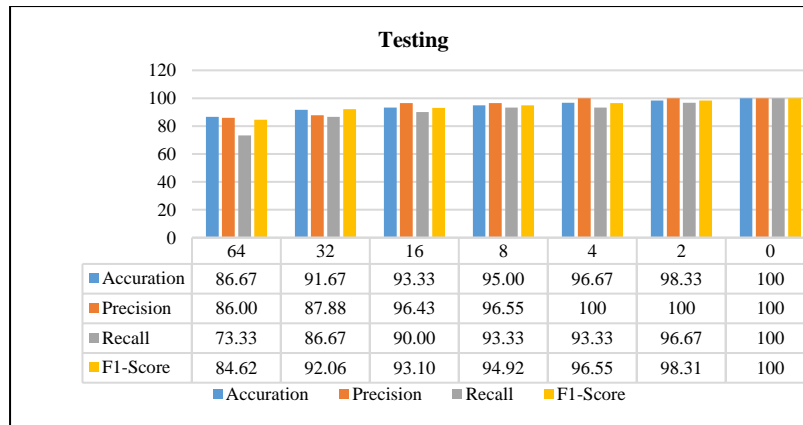


Figure 5. Testing Accuracy, Precision, Recall, and F1-Score at Different Compression Ratios

Table 2 shows a comparison of previous research with the proposed system. All studies carried out lung health classification using X-Ray images of the lungs with 2 classifications, namely normal lungs and infected with Covid-19. The comparison results show that the Alexnet model is superior to other architectures. When applying CS with CR=2, the proposed method has a performance that is not much different from other research, with the smallest Recall value of 96.67%.

Table 2. Comparison of Proposed System with Previous Studies

Reference	Methods	Accuracy	Precision	Recall	F1-score
Qjidaa, [25]	Ensemble	98.00%	98.66%	98.33%	98.30%
Barstugan et al., [26]	Feature Extraction + SVM	98.71%	99.62%	97.56%	98.58%
Ngesthi and Setyawan, [27]	Cropping + Resnet101	99.40%	98.70%	99.20%	99.00%

Altan, A. & Karasu, S, [28]	(2D) curvelet transformation, chaotic salp swarm algorithm (CSSA) and deep learning	99.69%	99.62%	99.44%	99.53%
Proposed	Alexnet	100%	100%	100%	100%
Proposed	CS (CR=2)+Alexnet	98.33%	100%	96.67%	98.31%

3.4. Discussion

3.4.1. Compressive Sensing Impact on PSNR

The application of CS techniques in this study demonstrated a significant impact on the Peak Signal-to-Noise Ratio (PSNR) of the compressed X-ray images. As shown in Table 1, a CR of 2 resulted in relatively high PSNR values for both COVID-19-affected and normal lungs, with 32.914 dB and 30.590 dB, respectively. This indicates that at lower compression, the image retains more of its original quality. However, as the CR increases, the PSNR drops substantially. At CR=64, the PSNR for COVID-19 images was 16.737 dB, while normal lung images dropped to 11.510 dB. This trend shows that higher compression ratios significantly degrade the image quality, making it difficult to discern details essential for accurate classification.

3.4.2. Effect on Image Quality

The visual analysis in figure 3 supports the numerical PSNR results. Images at lower CR values (figure 3(e) and figure 3(f)) maintain clarity, essential for diagnostic accuracy. However, at higher CRs (figure 3(a) and figure 3(b)), the images lose substantial detail, with only faint features visible. This observation confirms that while CS is useful for reducing file size, it comes at the cost of image fidelity. Therefore, there is a trade-off between file size and diagnostic utility, especially for medical images where fine details are crucial.

3.4.3. Training and Validation Accuracy

During the training phase, the system consistently achieved 100% accuracy across all iterations for 180 images. The model, based on the AlexNet architecture, demonstrated robust performance in learning patterns from the dataset, as seen in the training results. Validation accuracy also performed impressively, particularly when no compression or minimal compression was applied. However, with increasing compression ratios, validation accuracy showed some decline. This suggests that while the network can learn effectively from clear images, the performance is slightly impacted when image quality deteriorates due to compression.

3.4.4. Testing Performance and CS Impact

Testing results, as shown in figure 5, further highlight the system's efficacy across different compression scenarios. Without compression, the model achieved perfect scores, with 100% accuracy, precision, recall, and F1-score. At CR=2, the system maintained high performance with 98.33% accuracy, 100% precision, 96.67% recall, and 98.31% F1-score. This indicates that moderate compression does not severely impact the system's ability to classify lung conditions. However, as compression increases, these values gradually decline, emphasizing the importance of balancing compression levels with diagnostic accuracy.

3.4.5. Comparison with Previous Studies

Table 2 provides a comprehensive comparison of the proposed system's performance with prior research. Notably, the AlexNet architecture used in this study showed superior performance in classifying lung images without compression. This aligns with the findings of Ngesthi and Setyawan [27] also achieved high accuracy of 99.4% using ResNet101. The use of AlexNet in this study, with CS at CR=2, still achieved competitive results, demonstrating that even with moderate compression, the system retains considerable diagnostic power.

3.4.6. AlexNet's Superiority

The superior performance of AlexNet in this study, particularly in scenarios without compression, underscores the efficacy of this architecture in medical image classification tasks. AlexNet's ability to handle large datasets and extract meaningful features from X-ray images contributed to its high performance. Compared to other architectures like ResNet50, Ensemble models, and SVM-based methods, AlexNet demonstrated its robustness in achieving 100% across key classification metrics, as shown in table 2.

3.4.7. Compressive Sensing as a Trade-Off

While Compressive Sensing plays a crucial role in reducing file size, it introduces a trade-off in image quality. The study demonstrated that at CR=2, the system still produced reliable classification results, with minimal loss in diagnostic capability. However, as the CR increased, the model's classification ability diminished, particularly in terms of recall, which dropped to 96.67%. This trade-off needs to be carefully considered in practical applications, where both image size and classification accuracy are critical.

3.4.8. Challenges with Higher Compression Ratios

The results also highlight the challenges of employing higher compression ratios in medical imaging. As the compression ratio increased, the PSNR dropped, indicating significant degradation in image quality. This affected the network's ability to classify the images accurately, particularly when CR reached 64, where the recall and precision values dropped noticeably. These findings align with previous research by Barstugan et al. [26], which showed that feature extraction methods struggle when image quality is compromised due to aggressive compression.

3.4.9. Comparison with Feature Extraction Methods

Feature extraction techniques such as those used by Barstugan et al. [26] and Altan & Karasu [28] showed strong performance in earlier studies, particularly with the use of advanced methods like GLCM, GLSZM, and curvelet transformations. However, these methods tend to be more complex and computationally intensive compared to the AlexNet architecture used in this study. The current research demonstrates that AlexNet, combined with CS at moderate levels, can provide a simpler yet highly effective solution for lung image classification.

3.4.10. Future Directions and Improvements

The results of this study suggest that future research could explore optimizing the compression ratio to find a sweet spot that balances file size and classification performance. Further improvements could include experimenting with different deep learning architectures or hybrid methods to enhance classification accuracy at higher compression levels. Additionally, incorporating more diverse datasets could help generalize the model for broader clinical applications, making it a valuable tool in resource-constrained settings where file storage and transmission efficiency are crucial.

5. Conclusion

This research combines CS compression techniques and CNN classification applied to X-Ray images of lung health. The proposed method combines the CS method consisting of DCT, Gaussian measurement matrix, OMP reconstruction algorithm and CNN method in the form of the Alexnet architecture for classification of normal and Covid-19 infected lung images. The research tested the system with scenarios without compression and with compression using CR 2, 4, 8.16, 32, and 64. The results showed that the success of image compression using CR=2 and PSNR 27.715 dB, obtained classification parameters in the form of accuracy in training and validation of 100% and minimum test parameters of 96.67%. The Alexnet model was proven to be superior to other models in similar research. For further research, a mobile application will be created to detect lung health which can be used directly by interested parties, as well it will be developed for other types of lung disease.

6. Declarations

6.1. Author Contributions

Conceptualization: B.E.T., G.B., S.S.M., M.I.J., Y.S.H., I.D.I., Z.Z.; Methodology: S.S.M.; Software: B.E.T.; Validation: B.E.T., S.S.M., and I.D.I.; Formal Analysis: B.E.T., S.S.M., and I.D.I.; Investigation: B.E.T.; Resources: S.S.M.; Data Curation: S.S.M.; Writing Original Draft Preparation: B.E.T., S.S.M., and I.D.I.; Writing Review and Editing: S.S.M., B.E.T., and I.D.I.; Visualization: B.E.T and Z.Z. All authors have read and agreed to the published version of the manuscript.

6.2. Data Availability Statement

The data presented in this study are available on request from the corresponding author.

6.3. Funding

The authors received no financial support for the research, authorship, and/or publication of this article.

6.4. Institutional Review Board Statement

Not applicable.

6.5. Informed Consent Statement

Not applicable.

6.6. Declaration of Competing Interest

The authors declare that they have no known competing financial interests or personal relationships that could have appeared to influence the work reported in this paper.

References

- [1] G. Maschmeyer, "Pneumonia in febrile neutropenic patients: radiologic diagnosis," *Current opinion in oncology*, vol. 13, no. 4, pp. 229-235, 2001.
- [2] D. Biswas, A. Kumari, G. C. K. Chen, S. Vasudevan, S. Gupta, S. Shukla, and U. Garg, "Quantitative differentiation of pneumonia from normal lungs: diagnostic assessment using photoacoustic spectral response," *Applied Spectroscopy*, vol. 71, pp. 2532-2537, 2017.
- [3] S. A. Aljawarneh and R. Al-Quraan, "Pneumonia detection using enhanced convolutional neural network model on chest X-ray images," *Big Data*, vol. 2023, no. 1, pp. 1-6, 2023.
- [4] Z. Yang and Q. Zhao, "A multiple deep learner approach for X-Ray image-based pneumonia detection," in *2020 International Conference on Machine Learning and Cybernetics (ICMLC)*, vol. 2020, no. 7, pp. 70-75, 2020.
- [5] R. Kundu, R. Das, Z. Geem, G.-T. Han, and R. Sarkar, "Pneumonia detection in chest X-ray images using an ensemble of deep learning models," *PLoS ONE*, vol. 2021, no. 8, pp. 1-6, 2021.
- [6] M. Salehi, R. Mohammadi, H. Ghaffari, N. Sadighi, and R. Reiazi, "Automated detection of pneumonia cases using deep transfer learning with paediatric chest X-ray images," *The British journal of radiology*, vol. 2021, no. 1, pp. 1-7, 2021.
- [7] L. Valdes-Burgos, S. Contreras-Ojeda, J. A. Dominguez-Jimenez, J. Lopez-Bueno, and S. H. Contreras-Ortiz, "Analysis and classification of lung tissue in ultrasound images for pneumonia detection," in *Proceedings of SPIE Medical Imaging*, vol. 2020, no. 2, pp. 1-6, 2020.
- [8] S. Arunmozhi, V. Rajinikanth, and M. Rajakumar, "Deep-learning based automated detection of pneumonia in chest radiographs," in *2021 International Conference on System, Computation, Automation and Networking (ICSCAN)*, vol. 2021, no. 5, pp. 1-4, 2021.
- [9] K. More, P. Jawale, S. Bhattad, and J. Upadhyay, "Pneumonia detection using deep learning," in *2021 International Conference on Smart Generation Computing, Communication and Networking (SMART GENCON)*, vol. 2021, no. 6, pp. 1-5, 2021.
- [10] Z. Yang and Q. Zhao, "A multiple deep learner approach for X-Ray image-based pneumonia detection," in *2020 International Conference on Machine Learning and Cybernetics (ICMLC)*, vol. 2020, no. 7, pp. 70-75, 2020.
- [11] R. Kundu, R. Das, Z. Geem, G.-T. Han, and R. Sarkar, "Pneumonia detection in chest X-ray images using an ensemble of deep learning models," *PLoS ONE*, vol. 2021, no. 8, pp. 1-6, 2021.
- [12] Y. Demir, "Detection of pneumonia from pediatric chest X-Ray images by transfer learning," *Sigma Journal of Engineering and Natural Sciences*, vol. 2022, no. 1, pp. 1-6, 2022.
- [13] R. Hasan, S. M. A. Ullah, A. Nandi, and A. Taher, "Improving pneumonia diagnosis: A deep transfer learning CNN ensemble approach for accurate chest X-ray image analysis," in *2023 International Conference on Information and Communication Technology for Sustainable Development (ICICT4SD)*, vol. 2023, no. 3, pp. 109-113, 2023.
- [14] Y. Demir, "Detection of pneumonia from pediatric chest X-Ray images by transfer learning," *Sigma Journal of Engineering and Natural Sciences*, vol. 2022, no. 1, pp. 1-6, 2022.
- [15] Y. Wei, H. B. Hashim, S. H. Lai, K. L. Chong, Y. F. Huang, A. N. Ahmed, "Comparative Analysis of Artificial Intelligence Methods for Streamflow Forecasting," in *IEEE Access*, vol. 12, no. 1, pp. 10865-10885, 2024, doi: 10.1109/ACCESS.2024.3351754.

-
- [16] Y. Chung, N. Kim, D. Lee, S.-H. Kim, and J. Park, "Cough monitoring and pneumonia diagnosis algorithm through analysis of respiratory system-based vibro-acoustic signals and AI technology," *INTER-NOISE and NOISE-CON Congress and Conference Proceedings*, vol. 2021, no. 8, pp. 1-8, 2021.
 - [17] S. Mongodi, G. Via, M. Girard, I. Rouquette, B. Misset, A. Braschi, F. Mojoli, and B. Bouhemad, "Lung ultrasound for early diagnosis of ventilator-associated pneumonia," *Chest*, vol. 149, no. 4, pp. 969-980, 2016.
 - [18] S. A. Aljawarneh and R. Al-Quraan, "Pneumonia detection using enhanced convolutional neural network model on chest X-ray images," *Big Data*, vol. 2023, no. 1, pp. 1-6, 2023.
 - [19] Z. Yang and Q. Zhao, "A multiple deep learner approach for X-Ray image-based pneumonia detection," in *2020 International Conference on Machine Learning and Cybernetics (ICMLC)*, vol. 2020, no. 7, pp. 70-75, 2020.
 - [20] D. Biswas, A. Kumari, G. C. K. Chen, S. Vasudevan, S. Gupta, S. Shukla, and U. Garg, "Quantitative differentiation of pneumonia from normal lungs: diagnostic assessment using photoacoustic spectral response," *Applied Spectroscopy*, vol. 71, no. 12, pp. 2532-2537, 2017.
 - [21] Z. Yang and Q. Zhao, "A multiple deep learner approach for X-Ray image-based pneumonia detection," in *2020 International Conference on Machine Learning and Cybernetics (ICMLC)*, vol. 2020, no. 7, pp. 70-75, 2020.
 - [22] S. A. Aljawarneh and R. Al-Quraan, "Pneumonia detection using enhanced convolutional neural network model on chest X-ray images," *Big Data*, vol. 2023, no. 1, pp. 1-6, 2023.
 - [23] S. Mongodi, N. De Vita, G. Salve, S. Bonaiti, F. Daverio, M. Cavagnino, G. Siano, A. Amatu, G. Maggio, V. Musella, C. Klersy, R. Vaschetto, B. Bouhemad, and F. Mojoli, "The role of lung ultrasound monitoring in early detection of ventilator-associated pneumonia in COVID-19 patients: a retrospective observational study," *Journal of Clinical Medicine*, vol. 11, no. 6, pp. 1-6, 2022.
 - [24] Y. Chung, N. Kim, D. Lee, S.-H. Kim, and J. Park, "Cough monitoring and pneumonia diagnosis algorithm through analysis of respiratory system-based vibro-acoustic signals and AI technology," *INTER-NOISE and NOISE-CON Congress and Conference Proceedings*, vol. 2021, no. 8, pp. 1-8, 2021.
 - [25] M. Qjidaa, Y. Mechbal, A. ben-fares, H. Amakdoun, M. Maaroufi, B. Alami, and Q. Hassan, "Early detection of COVID-19 by deep learning transfer model for populations in isolated rural areas," *2020 International Conference on Smart Cities and Systems Engineering (ISCV)*, vol. 2020, no. 9, pp. 5-12, 2020, doi: 10.1109/ISCV49265.2020.9204099.
 - [26] M. Barstugan, U. Ozkaya, and S. Ozturk, "Coronavirus (COVID-19) classification using CT images by machine learning methods," *arXiv preprint*, arXiv:2003.09424, vol. 2020, no. 3, pp. 24-36, 2020, doi: 10.48550/arXiv.2003.09424.
 - [27] S. O. Ngesthi and I. Setyawan, "Optimized deep transfer learning for COVID-19 screening using chest X-ray image," in *2020 3rd International Conference on Information and Communications Technology (ICOIACT)*, vol. 2020, no. 3, pp. 6-13, 2020.
 - [28] A. Altan and S. Karasu, "Recognition of COVID-19 disease from X-ray images by hybrid model consisting of 2D curvelet transform, chaotic salp swarm algorithm and deep learning technique," *Chaos, Solitons and Fractals*, vol. 140, no. 1, pp. 10-21, 2020.